The 2009 IEEE/RSJ International Conference on
Intelligent Robots and Systems
October 11-15, 2009 St. Louis, USA

Stereovision-based Road Boundary Detection for Intelligent Vehicles in Challenging Scenarios

Chunzhao Guo, Seiichi Mita, *Member, IEEE*, and David McAllester, *Member, IEEE*

***Abstract*—Road detection is a crucial problem for intelligent vehicles and mobile robots. Most of the methods proposed nowadays only achieve reliable results in relatively well-arranged environments. In this paper, we proposed a stereovision-based road boundary detection method by combining homography estimation and MRF-based belief propagation to cope with challenging scenarios such as unstructured roads with unhomogeneous surfaces. In the method, each pixel in the reference image is firstly labeled as "road" or "non-road" by minimizing a well defined energy function that accounts for the planar road region. Subsequently, both of the road boundaries are generated using Catmull-Rom splines based on RANdom SAmple Consensus (RANSAC) algorithm with varying road structure models to help the intelligent vehicle understand the structure as well as safe range of current road. In the suggested framework, both intensity and geometry information of road scenarios are used to contain all the regions belonging to the planar road plane, and the left and right road boundaries are generated separately using a robust fitting algorithm to handle different road structures. Therefore, more accurate as well as robust detection of the road can be expected. Experimental results on a wide variety of typical but challenging scenarios have demonstrated the effectiveness of the proposed method.**

I. Introduction

ROAD detection is a crucial problem for intelligent vehicles and mobile robots. It provides information about the world that enables the intelligent vehicle or robot to interact with its environment and react to events or changes that influence its task [1]. Many researchers have been studying it for several decades and dramatic development has been accomplished, which can be categorized into two main types of methods: vision-based methods [2]-[7] and LIDAR-based methods [8]-[10]. While typical systems make use of cameras as well as LIDAR sensors [11] and have been proved to be highly applicable in practice because LIDARs can directly measure range, it is possible to make use only of cameras for both range and color information, just like human drivers/operators. Therefore, vision-based road detection is a very important as well as promising branch in the field. Among the current vision-based methods, some use monocular camera to extract the road region by employing features with specific intensity, color and texture as visual cues on the road surface [2]-[4]. Others use binocular camera (or more cameras) for road detection by utilizing 3D structural information [5]-[7]. Most of the methods proposed nowadays only achieve reliable results in relatively well-arranged environments; however, there are still many unstructured roads with unhomogeneous surfaces in the real world environments, such as rural roads and campus roads etc. In these typical but challenging scenarios, both intensity and geometry information should be used since different parts of the road surface may have totally different intensities; however, each part should be contained in the detected road as long as it belongs to the same planar road plane that vehicles can pass safely.

The proposed method is developed in the scope of the stereovision-based navigation system integrated in our experimental intelligent vehicle shown in Fig. 1, which is equipped with six computers and various sensors (stereo camera, laser scanner, all round camera, GPS, etc). It is designed to detect the drivable road region and generate road boundaries to help the host vehicle understand the structure as well as safe range of current road and make the correct decision to drive in a safe path. Here, we define the drivable road region as a connected region in front of the vehicle on the road plane where a vehicle can pass safely, under the flat-road assumption.

Figure 1. Our experimental intelligent vehicle

The main idea of the proposed method is to assign each pixel in the reference image a label (1 for road region and 0 for non-road region) by minimizing a well defined energy function that accounts for the planar road region. The energy function is defined by utilizing the 2D projective transformations of stereo information and the inference algorithm in binary piecewise Markov Random Field (MRF). It has two terms: one term penalizes solutions that are inconsistent with the observed data, whereas the other term enforces spatial coherence (piecewise smoothness). Subsequently, Road boundaries are generated separately using Catmull-Rom splines based on RANdom SAmple Consensus (RANSAC) algorithm with varying road structure models to help the intelligent vehicle understand the structure as well as safe range of current road.

The rest of the paper is organized as follows: Section II gives the outline of the proposed method. The detailed description of the MRF-based drivable road region detection method is presented in section III. Section IV explains the

Manuscript received February 25, 2009. This work was supported by the Research Center for Advanced Intelligent Systems and Devices of Toyota Technological Institute, Japan. Partner institutions are the Toyota Technological Institute at Chicago, USA, and Toyota Central R&D Labs, Inc., Japan.

Chunzhao Guo and Seiichi Mita are with the Toyota Technological Institute, Nagoya, Aichi 468-8511 Japan. (e-mail: {guo, smita}@toyota-ti.ac.jp).

David McAllester is with the Toyota Technological Institute at Chicago, Chicago, IL 60637 USA. (e-mail: mcallester@tti-c.org).

road boundaries generation. The experimental results on real typical but challenging road scenarios are given in section V, which have demonstrated the effectiveness as well as robustness of the proposed method. Finally, the conclusion is drawn in section VI.

II. Outline of the Proposed Method

In the projective geometry of two cameras and a world plane, images of points on a plane are related to corresponding image points in a second view by a planar homography as shown in Fig. 2 [12]. The map from the point x to x' is the homography H induced by the plane π. Between the image planes, there is

$$x' = Hx \tag{1}$$

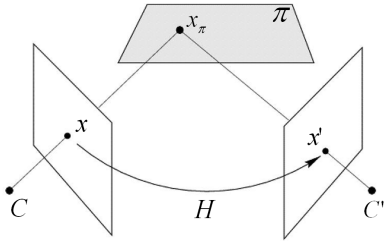

Figure 2. The homography induced by a plane.

As for road detection, when we assume that the drivable road region is a planar plane, we can use the homography induced by the road plane to transform the image from one view to the other. When the transformed image is then compared against the reference image, only the points on the road plane can coincide very well while other points that elevate out from the road appear distorted, according to (1). Therefore, all the regions belonging to the same planar road plane should be contained in the matched area no matter how big their intensity differences are. In this case, the drivable road region detection is actually a simple form of the stereo matching problem. It just needs to find the matched pixel locations, which will be regarded as the detected road region, between the transformed image and the reference image, instead of finding the correspondences for every pixel.

Fig. 3 shows the flow diagram of the proposed method. Firstly, MRF-based road detection is performed, in which, drivable road detection is defined as a binary labeling. The binary labeling is optimized by minimizing a well defined energy function that accounts for the planar road region. The energy is minimized in coordinate descent iterations that alternate between optimizing the homography induced by the planar road plane for 2D projective transformations and implementing efficient belief propagation to find the optimal binary labeling that segments the image into two non-overlapping road and non-road regions. Secondly, both of the road boundaries are generated separately using Catmull-Rom splines based on RANSAC algorithm with varying road structure models to help the intelligent vehicle understand the structure as well as safe range of current road. In this step, roadside pixels are extracted, and then line segments are grouped as well as selected for fitting. Meanwhile, the skeleton of detected road is also extracted to determine the number of control points of the splines according to different road structure models. In the suggested framework, both intensity and geometry information of road scenarios are used to contain all the regions belonging to the planar road plane, and the left and right road boundaries are generated separately using a robust fitting algorithm to handle different road structures. Experimental results on a wide variety of typical but challenging scenarios have demonstrated the accuracy as well as robustness of the proposed method.

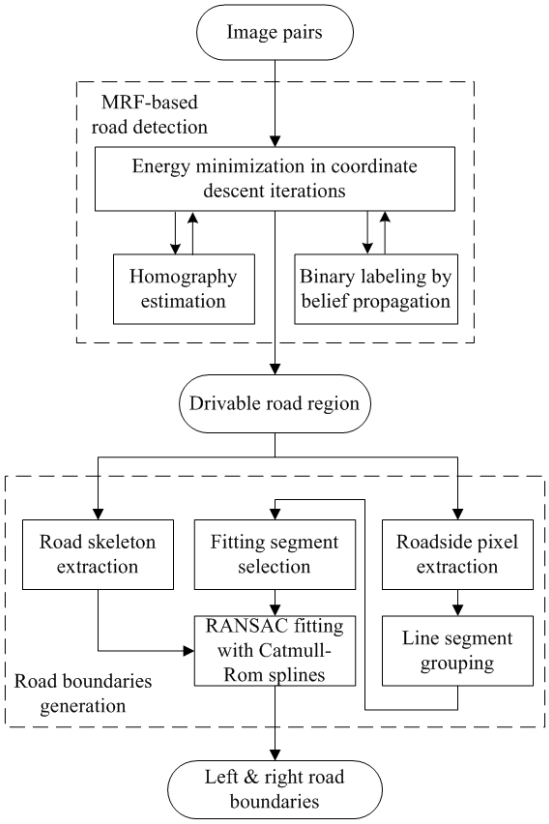

Figure 3. Flow diagram of the proposed method

Textureless regions that connect to the road region, such as black cars, white walls, etc., may frequently cause misdetections, since the intensities do not change in some parts of the textureless region although their positions changed. In order to solve this problem, all textureless regions in the input image pair are extracted and their contours are recorded. Only the regions whose contours in the transformed image and the reference image coincide well will be preserved in the drivable road region. The disagreements of the other regions' contours indicate they do not belong to the road plane. Therefore, these regions will be labeled as non-road regions. The parts of non-road regions included in the extracted drivable road region will be removed, although the intensity patterns coincide well.

III. MRF-based Drivable Road Region Detection

MRF models provide a robust and unified framework for stereo problems. An important component of MRF-based approaches is the inference algorithm used to find the most likely setting of each node in the MRF. Therefore, we formulate the drivable road detection as a MRF model and implement an efficient belief propagation approach to obtain the Maximum A Posteriori (MAP) estimation in the MRF, since the MAP-MRF approach has proven to be extremely successful for many vision applications [13].

A. Dynamic Homography Estimation

Many stereovision-based road detection methods assume that the cameras are calibrated beforehand and the

geometrical relations between cameras and the road plane are known and fixed. However, these assumptions are not practical in real applications because the vehicle may tilt and the cameras may vibrate. Therefore, the geometrical relations, e.g. the homography induced by the road plane in the proposed method, must be estimated and updated dynamically for each and every frame in order to achieve more accuracy as well as robustness. Feature-based methods can estimate the homography accurately based on the correspondences of feature points on the road plane. However, once some mismatching happens to the correspondences, the result will be affected. Therefore, we employ an area-based method for the estimation of homography. In this case, the point-to-point correspondences are not necessary and the matching is optimized using all pixel information in a predicted road region, which is derived from temporal information of the input image pairs based on Markov chains. Therefore, more accurate as well as robust detection of the road region can be expected.

In the present case, we are seeking a homography H that minimizes the total intensity error function $E(H)$ in (2) between the image pair,

$$e(H) = \sum_{x \in Rp} | I_l(x) - I_r(Hx) | \quad (2)$$

where, I_l, I_r are the left and right image, respectively, Rp is the predicted road region. This region is actually derived from the detected drivable road region of the adjacent previous image, by transforming it with the predefined homography between sequential images according to the current driving state. The current driving state can be obtained from the control system of the host vehicle, or ego-motion estimation if communication with the control system is not available.

B. MRF-based Drivable Road Region Detection

In the MRF, given the transformed image and the reference image, we present the road detection as a binary labeling $f : x \to \{0,1\}$ for each pixel x at pixel location p in the reference image, and the assigned label denoted by a random variable f_p is

$$f_p = \begin{cases} 1 & p \in \text{Drivable road region} \\ 0 & \text{Otherwise} \end{cases} \quad (3)$$

Our goal is to find the correspondence that matches pixel locations of similar intensity while minimizing the number of discontinuities, since the labels should not vary in either road or non-road region but just change at pixel locations along the boundary between the two regions. We accomplish this by minimizing the following energy function, which describes the quality of labeling,

$$E(f) = \sum_{p \in P} D_p(f_p) + \sum_{(p,q) \in N} V(f_p, f_q) \quad (4)$$

where P is the set of pixels in the reference image. N are the undirected edges in the 4-connected image grid graph. $D_p(f_p)$ is the cost of assigning label f_p to pixel p, and is referred to as the data term. $V(x_p, x_q)$ measures the cost of assigning labels f_p and f_q to two neighboring pixels, and is referred to as the smoothness term.

In the proposed method, we define the data term as

$$D_p(f_p) = | I_l(p) - I_{tr}(p) | f_p + c(1 - f_p) \quad (5)$$

where I_l, I_{tr} are the intensities in the reference image and transformed image, respectively. c is a thresholding factor to adjust the influence of the intensity difference on the labeling. In order to minimize the data term, f_p will be assigned with 1 if the intensity difference is smaller than c. Otherwise the variable will be assigned with 0. In stereo problems, the smoothness term is generally based on the difference between labels, rather than on their actual values. Therefore, we define the smoothness term as

$$V(f_p, f_q) = \lambda | f_p - f_q | \quad (6)$$

where λ is a scaling factor. The smoothness term enforces smoothness by penalizing the discontinuities. $V(x_p, x_q)$ is equal to 0 for the neighboring pixels belonging to the same road or non-road region and λ for the pixels along the boundary between the two regions. Finding a labeling that minimizes this energy corresponds to the MAP estimation for the MRF defined as above.

C. Combination of Dynamic Homography Optimization and MRF- based Road Detection

The optimized homography is used to transform an image from one view to the other, which is then compared against the reference image. Therefore, it is only related to the data term. We combine the dynamic homography estimation and the MRF-based road detection in the proposed method by re-defining the data term as

$$D_p(f_p) = | I_l(p) - I_r(Hp) | f_p + c(1 - f_p) \quad (7)$$

where I_l, I_r are the intensities in the left and right image, respectively. The energy in (4) with the new data term is minimized in coordinate descent iterations [14] that alternate between optimizing the homography and implementing an efficient belief propagation approach [15] to find the optimal binary labeling that segments the image into two non-overlapping road and non-road regions. The optimization procedure is initialized by a feature-based road detection method [16], in which, the homography is estimated by corresponding corner points lying on the road plane between the first stereo image pair and the drivable road region is extracted using the SAD matching technique with the transformed image and the reference image.

It should be noted that the homography is only optimized at pixels where $f_p = 1$. Therefore, the optimized homography is purely induced by the road region, which ensured the accuracy of the estimation of homography.

IV. ROAD BOUNDARIES GENERATION

The goal of road detection is to build and maintain the representation of the world that the behavior generation components of the intelligent vehicle or mobile robot can use to plan and execute actions [1]. Therefore, in the proposed method, both of the road boundaries are generated separately based on the obtained drivable road region, using Catmull-Rom splines with RANSAC algorithm to help the intelligent vehicle understand the structure as well as safe range of current road. Note that we generate the left and right boundaries separately, unlike much of the previous work which has a road model of uniform width, to deal with various scenarios such as roads with branches or varying width.

Splines are smooth piecewise polynomial functions, and they are widely used in representing curves. Various spline

representations have been proposed, and we use the Catmull-Rom spline among them because its control points are actually on the curve and it has local control, which means that modifying one control point only affects the part of the curve near that control point. These characteristics enable fast fitting of the curve. Given a series of positions $(P_0, P_1, ..., P_n)$, the Catmull-Rom spline is able to interpolate (pass through) the points from P_1 to P_{n-1}. In addition, the tangent vector at P_i is parallel to the line connecting P_{i-1} and P_{i+1}.

The formula is Catmull-Rom spline for one segment is [17]:

$$P(t) = \frac{1}{2}[t^3 \quad t^2 \quad t \quad 1]\begin{bmatrix} -1 & 3 & -3 & 1 \\ 2 & -5 & 4 & -1 \\ -1 & 0 & 1 & 0 \\ 0 & 2 & 0 & 0 \end{bmatrix}\begin{bmatrix} P_{i-3} \\ P_{i-2} \\ P_{i-1} \\ P_i \end{bmatrix} \quad (8)$$

where P_i is the control point which requires the Catmull-Rom spline to pass through, $t \in [0,1]$.

The main behavior generation component of a driving intelligent vehicle is the steering system. Therefore, the general situations of understanding the structure of the road for decision making mainly include four fundamental road structure models, i.e. straight ahead road, left bound road, right bound road and branch road. For the first three non-branch roads, two independent Catmull-Rom splines with five control points are eligible to describe the left and right road boundaries. For the branch road, the Catmull-Rom spline with six control points is used to describe the boundary with branch. Here, we set the first and the last two control points equal for each spline since the Catmull-Rom spline interpolates all but the first and the last control points. Therefore, each boundary is actually determined by three control points for non-branch roads and four control points for branch roads.

Once the drivable road region is detected, its skeleton is extracted to judge whether the current road is a branch road or not, and determine the number of control points as well. Subsequently, pixels on both lateral sides of its contour are extracted and the line segments, excluding the nearly horizontal segments and segments lying in the image borders, are grouped into two independent sets to fit the Catmull-Rom splines for the left and right road boundaries, respectively. More formally, a line segment AB lying outside the image borders will be preserved for the spline fitting if

$$\left|\frac{y_A - y_B}{x_A - x_B}\right| > \delta \quad (9)$$

where x_A, y_A, x_B, y_B are coordinates of the end points and δ is a threshold to exclude the nearly horizontal line segments.

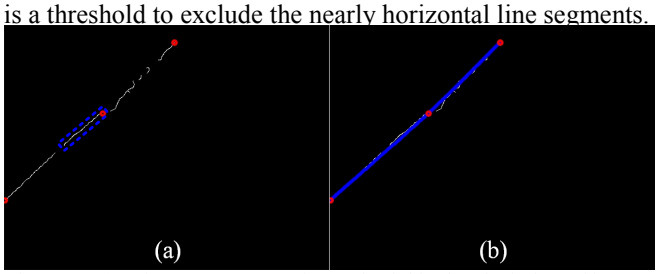

Figure 4. (a) Line segment grouping and neighborhood window of interest (b) fitting result using RANSAC algorithm

The RANSAC algorithm is then applied to each preserved line segments set to generate the road boundary using Catmull-Rom spline by repeating the following procedures N times, with an example of left boundary generation shown in Fig. 4.

a) Select a random sample of line segments.

b) Fit a Catmull-Rom spline with the selected sample segments using the least squares method. For each of the selected sample segments, we define a neighborhood window of interest around it. The first (nearest) control point is forced to be on the side border of the image due to the camera configuration. The last (farthest) control point is set to the end point of the farthest line segment. The other control points are searched in the neighborhood windows of interest. The positions of control points that minimize the sum of squared error of fitting the sampled points will be preserved as the fitting result. The initial positions of the control points are derived from the adjacent previous image, by moving the previously detected boundary's control points according to the current driving state.

c) Calculate the score of the fitted spline and check the inliers. In normal RANSAC algorithm, the score that indicates the goodness of the fit is obtained by calculating the normal distance from each point to the fitted spline. However, it has to solve a quintic equation for each and every point. Here, we implement a more efficient approach [18] to calculate the score of the fitted spline by rasterizing it and then counting the values of pixels belonging to the spline.

d) Update the spline (positions of control points) and the inliers set if the number of inliers for the spline is maximum.

e) Update N.

The use of RANSAC algorithm for fitting the road boundaries enables an accurate as well as robust road boundary generation even when significant amount of outliers are present in the drivable road region detection.

V. Experimental Results

In the experiments, the proposed method has been implemented in C++ on Microsoft Windows using the OpenCV library. The gray scale road image sequences on a wide variety of typical but challenging scenarios were tested on a Core2 Dual 3.0 GHz PC without code optimization, which are from three video clips of 640×480 image resolution. The Canny edge detector [19] is performed in the original input image pair, and the superimposed images of the original images and the edge images are input and processed in the road detection. The aims of this step are: a) to obtain the textureless regions in the images, due to the reason explained in section II; b) to enhance the edge evidence while maintaining the texture information. The enhanced edge can prevent connections of the regions in the result image that are actually unconnected for a human observer as much as possible. The average computational time was under 550 ms/frame. The computational time will be further reduced to satisfy the real-time detection for the experimental vehicle by utilizing special image processing hardware, reducing the image resolution as well as optimizing the codes of the proposed method.

Here, we mainly focused on various typical but challenging scenarios with different complicated road

appearances and weather conditions, such as multi-colored paved road, dirt roads with brushwood, and sunny roads with heavy shadows, etc. Example results of ten image sequences are shown in Fig. 5, in which, the detected drivable road region is indicated by the highlight area and road boundaries are indicated by the blue splines with three or four red control points. The left column shows the first images of the sequences, the middle column shows the detected results of the first images, and the right column shows the detected results of the last images of the sequences. None of the example roads has homogeneous surface. Fig. 5(a) shows the results on a left bound turnoff road with traffic signs on the surface. The Catmull-Rom spline with four control points is used to describe the left road boundary. Fig. 5(b) shows the results on a straight ahead road where only the right border exists and many cars parked on the left of the road. Fig. 5(c) shows the results of a right turn of the vehicle in an intersection where the border between the lawn and the road is very low. There are no road boundaries generated because the line segments on both sides of its contour belong to the image borders so that there is no line segments preserved. Fig. 5(d) shows the results on a multi-colored paved road with a passing vehicle, which is detected and excluded from the drivable road region as well as the right road boundary. Fig. 5(e) shows the results on an even more complicated multi-colored paved unflat road. The textureless pillars that connected to the road region were excluded. Fig. 5(f) shows the results of a slanted planar road with many complex intensity patterns on the surface, which substantiated that the proposed method can overcome the sensitivities brought by complex unhomogeneous road surfaces by the belief message propagating through neighbors. Fig. 5(g) shows the results on a dirt road with poorly-defined borders. There are many cars on the left side of the road and short brushwood on the right side of the road. Fig. 5(h) shows the results of a right bound dirt road with many faded leaves and grass on the surface. Fig. 5(i) shows the results on a sunny road with heavy shadows of buildings and trees as well as a passing bicycle. Both the sunny road region and the shadowed road region were included in the drivable road region, only the borders between the sunny and shadowed regions are missed due to the strong edge. Fig. 5(j) shows the results on an urban road at night, where there are both leading and passing vehicles with open lamps. While the right white line is missed in the drivable road region detection due to the strong edge, the right road boundary is generated along the white line due to the preserved line segments. In the typical but challenging scenarios shown in Fig. 5 we can see that, the drivable road region as well as road boundaries are basically in good agreement with the real situation. The generated road boundaries can reveal the structure as well as safe range of current road so that the intelligent vehicle can understand it and make the correct decision to drive in a safe path.

Furthermore, quantitative evaluations as well as a comparison with road detection method using SAD matching [16] with the ten image sequences are given in Table I. For the example images in the sequences, the pixels were manually labeled by a human operator, which is taken as the ground truth labeling. The automatic detection results are quantitatively evaluated according to three ratios: the false positives ratio (FPR), the false negatives ratio (FNR) and the accuracy, which are defined as follows:

$$\mathrm{FPR} = \frac{\sum_{i \in S} FP_i}{\sum_{i \in S} P_i} \times 100\% \qquad (10)$$

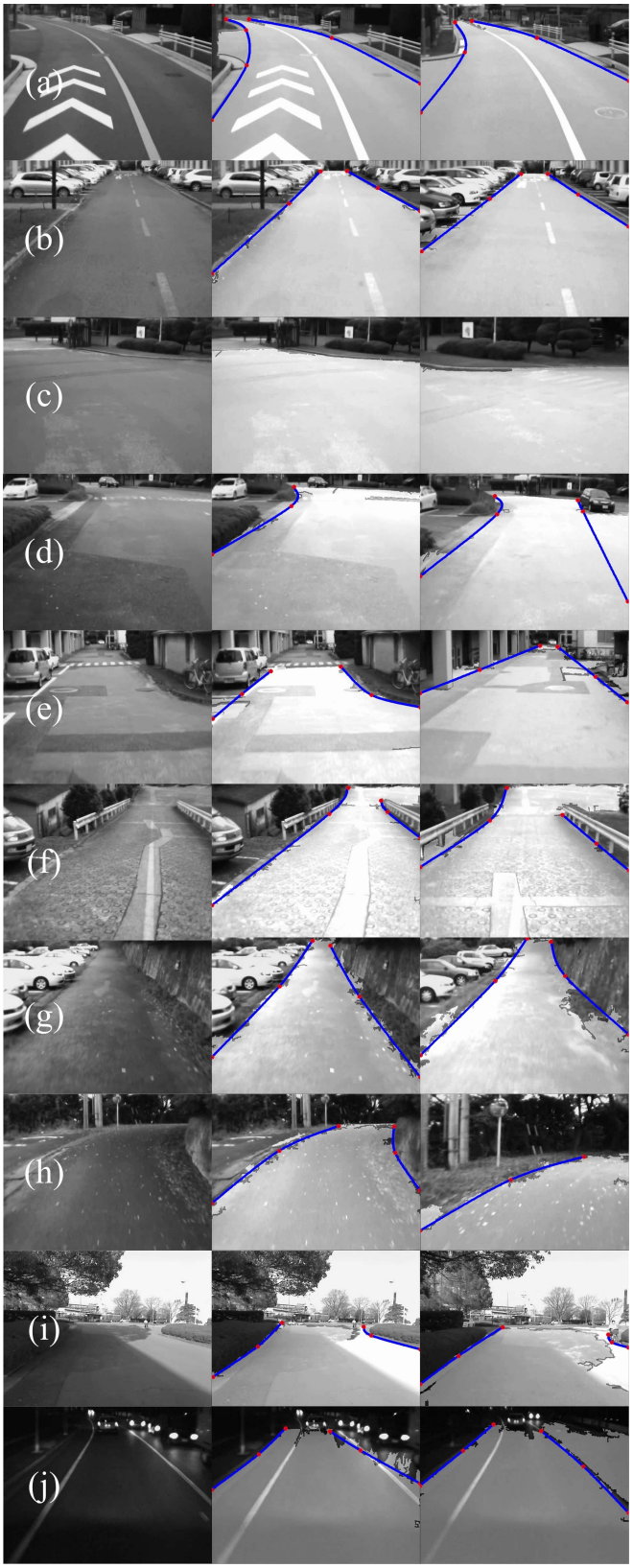

Figure 5. Example detection results. (a) left bound turnoff road (frames 117, 130), (b) straight ahead road (fames 485, 507), (c) right turn (frames 396, 423), (d) multi-colored paved road (frames 272, 307), (e) multi-colored unflat road (frames 799, 830), (f) slanted planar road (frames 1043, 1067), (g) dirt road (frames2012, 2048), (h)right bound dirt road (frames 2099, 2124), (i) sunny road with shadows (frames482, 504). (j) night view road (frames 48, 89).

$$\text{FNR} = \frac{\sum_{i \in S} FN_i}{\sum_{i \in S} N_i} \times 100\% \quad (11)$$

$$\text{Accuracy} = (1 - \frac{\sum_{i \in S} (FP_i + FN_i)}{\sum_{i \in S} (P_i + N_i)}) \times 100\% \quad (12)$$

where, S indicates an image sequence, FP_i is the number of non-road pixels erroneously labeled as road (false positives) in the i^{th} image, P_i is the number of road pixels in the i^{th} ground truth labeling, FN_i is the number of road pixels erroneously labeled as non-road (false negatives) in the i^{th} image and N_i is the number of non-road pixels in the i^{th} ground truth labeling. Table I shows the detection accuracy of the proposed method is satisfying and better than the method using SAD matching, especially for the roads with complex unhomogeneous surfaces.

TABLE I. QUANTITATIVE EVALUATIONS OF THE IMAGE SETS USING THE PROPOSED MEHTOD AND METHOD USING SAD MATCHING

	Method using SAD matching			The proposed method		
	FPR (%)	FNR (%)	Accuracy (%)	FPR (%)	FNR (%)	Accuracy (%)
(a)	1.521	1.913	98.372	0.456	0.714	99.474
(b)	1.502	4.689	97.688	0.732	1.316	99.119
(c)	1.137	4.756	97.819	0.606	2.584	98.823
(d)	1.024	40.215	89.122	0.832	7.760	97.426
(e)	4.112	45.172	84.843	1.142	12.901	95.695
(f)	6.642	49.523	82.624	1.337	1.436	98.639
(g)	5.670	25.702	85.931	2.932	0.394	98.132
(h)	5.026	24.581	85.799	0.840	1.309	98.940
(i)	2.037	28.312	83.123	1.170	1.841	98.451
(j)	2.113	29.687	90.996	0.350	11.138	96.954

Both Fig. 5 and Table I have demonstrated the accuracy as well as robustness of the proposed method.

VI. CONCLUSION

In this paper, we proposed a stereovision-based road boundary detection method to cope with challenging scenarios such as unstructured roads with unhomogeneous surfaces. The drivable road region is detected by minimizing a well defined energy function that accounts for the planar road region in the MRF by utilizing both intensity and geometry information of the road scenarios. Spline-based road boundaries are generated separately based on RANSAC algorithm with varying road structure models to help the intelligent vehicle understand the structure as well as safe range of current road. The use of RANSAC algorithm in road boundary generation can correct the errors by removing outliers if misdetection is present in the previous detected drivable road region. Therefore, the proposed method can be expected to be more accurate as well as robust. Experimental results on a wide variety of typical but challenging real road scenes have demonstrated the effectiveness of the proposed method.

REFERENCES

[1] R. Madhavan, E. Messina, and J. Albus, Intelligent Vehicle Systems A 4D/RCS Approach. New York: Nova Science Publishers Inc., 2006.

[2] M. Bertozzi, A. Broggi, and A. Fascioli, "Vision-based intelligent vehicles: State of the art and perspectives," *Robot. Autonom. Syst.*, vol. 32, pp. 1–16, 2000.

[3] Y. He, H. Wang, and B. Zhang, "Color-based road detection in urban traffic scenes," *IEEE Trans. on Intelligent Transport System*, Vol. 5, No. 4, 2004, pp. 309-318.

[4] P. Jeong and S. Nedevschi, "Efficient and Robust Classification Method Using Combined Feature Vector for Lane Detection," *IEEE Transaction on Intelligent Transportation System*, Vol. 15 No. 4, APRIL 2005.

[5] P. Lombardi, M. Zanin, and S. Messelodi, "Unified stereovision for ground, road, and obstacle detection," in *Proc. IEEE Intelligent Vehicles Symp.*, Las Vegas, USA, June 2005, pp. 783-788.

[6] N. Hautiere, R. Labayrade, M. Perrolaz, and D. Aubert, "Road scene analysis by stereovision: a robust and quasi-dense approach," in *Proc. of the Ninth International Conference on Control, Automation, Robotics and Vision*, Singapore, Dec. 2006, pp. 1-6.

[7] M. Okutomi, K, Nakano, J. Maruyama, and T. Hara, "Robust estimation of planar regions for visual navigation using sequential stereo images," in *Proc.of the 2002 IEEE International Conference on Robotics & Automation*, Washington, DC, May 2002, pp. 3321-3327.

[8] B. Fardi, U. Scheunert, H. Cramer, and G. Wanielik, "Multi-modal detection and parameter-based tracking of road borders with a laser scanner," *Proc. IEEE Intelligent Vehicles Symposium*, 2003, pp. 95 - 99.

[9] A.V. Reyher, A. Joos, H. Winner, "A lidar-based approach for near range lane detection," *Proc. Conf. on Intelligent Vehicles Symposium*, 2005, pp. 147 - 152.

[10] J. Sparbert, K. Dietmayer, D. Streller, "Lane detection and street type classification using laser rangeimages," *Proc. IEEE Conf. on Intelligent Transportation Systems*, 2001, pp. 454 - 459.

[11] C. Rasmussen, "Combining laser range, color, and texture cues for autonomous road following," *Proc. Int. Conf. on Robotics and Automation*, 2002, pp. 4320-4325.

[12] R. Hartley, and A. Zisserman, Multiple View Geometry in Computer Vision. Cambridge, UK:Cambridge University Press, 2003.

[13] C. Rother, V. Kolmogorov,V. Lempitsky, and M. Szummer, "Optimizing Binary MRFs via Extended Roof Duality", in *CVPR'07*, Jun. 2007, pp. 1-8.

[14] Y. Zakharrov, and F. Albu, "Coordinate Descent Iterations in Fast Affine Projection Algorithm," in *IEEE Signal Processing Letters*, Vol. 12, No. 5, 2005, pp. 353-356.

[15] P. Felzenszwalb, and D. Huttenlocher, "Efficient Belief Propagation for Early Vision," in *CVPR'04*, Jun. 2004, pp. 261-268.

[16] C. Guo, and S. Mita, "Drivable Road Region Detection based on Homography Estimation with Road Appearance and Driving State Models," in *ICARA'09*, Feb. 2009, pp. 204-209.

[17] Foley, Van Dam, Feiner, Hughes, Computer Graphics: Principles and Practice. Second Edition, Addision-Wesley Publishing Company,1990.

[18] David Solomon, Curves and Surfaces for Computer Graphics, Springer, 2006.

[19] J. Canny, "A Computational Approach to Edge Detection," in *IEEE Trans. Pattern Analysis Machine Intelligence*, 1986, pp. 679-714.